Structure and Dynamics of Water Confined in a Boron Nitride Nanotube

Chang Y. Won and N. R. Aluru*

Department of Mechanical Science and Engineering, Beckman Institute for Advanced Science and Technology, University of Illinois at Urbana-Champaign, Urbana, Illinois 61801

Received: August 22, 2007; In Final Form: October 23, 2007

Recent molecular dynamics simulations have shown that a finite-length (5,5) boron nitride nanotube (BNNT) in contact with an aqueous reservoir has superior water permeation properties compared to a (5,5) carbon nanotube of similar diameter and length. In this work, by using density functional theory (DFT), we compute the electrostatic potential arising from the weak ionic and covalent bonding of B−N. Quantum partial charges of B and N atoms, determined by matching the electrostatic potential computed by the DFT, are then included in molecular dynamics simulations to investigate the structure and dynamics of water confined in BNNTs of sizes ranging from (5,5) to (10,10). When partial charges are included, we observe that the wetting behavior of the (5,5) BNNT has improved and the single-file water chain in both (5,5) and (6,6) BNNTs has an *L*-defect. Further, with partial charges, except for a (9,9) BNNT which exhibits anomalous behavior, the diffusion coefficient of confined water molecules in (5,5), (6,6), and (10,10) BNNTs is found to decrease due to the formation of a hydrogen bond between water and nitrogen atoms. For a (9,9) BNNT, in the absence of partial charges, an ice-shell structure was observed with a critical slowing in the diffusion coefficient. When partial charges are included, the diffusion coefficient is found to increase because of the presence of an additional single-file water chain inside the ice-shell structure.

1. Introduction

Carbon nanotubes (CNTs) have been investigated extensively over the past decade for various applications due to their unique electrical and mechanical properties. Soon after the discovery of CNTs, efforts were made to search for a nanotube made of non-carbon material. In 1994, Blasé and his co-workers[1] predicted theoretically the boron nitride nanotube (BNNT) by exploring the similarity between hexagonal boron nitride and graphite. The existence of BNNTs was later confirmed by experimental synthesis.[2] BNNTs exhibit appealing properties such as a large electronic band gap, mechanical strength, and chemical inertness. Thus, BNNTs have attracted considerable attention recently.

BNNTs possess many of the superior properties of CNTs such as high material stiffness[3,4] (estimated Young's modulus is 1.1−1.3 TPa) and high heat conduction[5] (estimated thermal conductivity is ∼300 W/mK at 300 K). BNNTs exhibit semiconducting properties with wide band gap values (∼5.5 ev) nearly independent of their chirality and diameter.[1] Recently, it has been reported that the band gap of BNNTs can be tuned through a transverse electric field or covalent functionalizations.[6,7] This opens up many new applications of BNNTs, for example, as electro-optical devices. Beyond the electronic properties, the high-temperature resistance of a BNNT to oxidation makes the tube particularly useful for applications at high temperature. A BNNT is stable up to ∼700 °C in air, and the onset temperature for oxidation of a BNNT is ∼800 °C;[8] CNTs are oxidized in air at ∼400 °C, and they are completely burnt at ∼700 °C with a continuous oxygen supply.[9,10] These exciting properties allow BNNTs to be complementary materials to CNTs or even to replace the CNTs for applications requiring chemical stability, high-temperature resistance, or electrical insulation.

Since Hummer et al.[11] revealed that water permeates a single-walled carbon nanotube (SWCNT), extensive studies have been performed on understanding the structure and dynamics of water inside a SWCNT.[12] Due to the comparable size of a SWCNT to a biological ion channel,[13] a SWCNT has been considered to have great potential for applications in biological nanosystems. Because of their exciting properties, BNNTs can also find interesting applications in biological nanofluidic systems. Won and Aluru[14] recently reported that comparatively strong interactions between N atoms on a BNNT and water molecules induce a favorable filling of an empty finite-length (5,5) BNNT with water molecules. Furthermore, the diffusion coefficient of water molecules in a finite-length (5,5) BNNT is comparable to that in a (6,6) CNT. These superior filling and transport properties of water in a subnanometer BNNT suggest that a BNNT can be an excellent water conductor. However, there have been no reported studies so far on water structural and transport properties in a BNNT.

In this study, the structure and dynamics of water confined within a finite-length BNNT of various diameters are investigated using molecular dynamics (MD) simulations. The difference in electronegativity between boron and nitrogen atoms results in a combination of weak ionic and covalent bonding in a boron nitride nanotube.[15] Since classical molecular dynamics typically does not capture the polarization of a BNNT arising from its unique bonding nature, we perform density functional theory (DFT) calculations to capture the polarization effects. The partial charges computed from DFT calculations are used in molecular dynamics simulations to scrutinize their effect on water structure and transport. The rest of the paper is outlined as follows. First, DFT calculations and MD simulations will be described. The atomic partial charges computed from DFT are then summarized. The comparison of single-file water structure and orientation inside a BNNT and a CNT is discussed. Then

* Corresponding author. E-mail: aluru@uiuc.edu.

10.1021/jp076747u CCC: $40.75
Published on Web 01/24/2008

the combined effect of confinement and atomic partial charges on water structure and transport properties is discussed, followed by conclusions.

2. Methods

We performed DFT calculations and MD simulations on open-ended finite-length BNNTs of various diameters. Specifically, we considered open-ended (5,5), (6,6), (9,9), and (10,-10) BNNTs with a length of about 14 Å. The diameter of BNNTs ranges from 6.9 to 13.6 Å. The tubes are saturated at the ends with hydrogen atoms. The initial BN bond length was 1.446 Å. The N−H and B−H bond length was 1.09 Å. The N atoms were then moved slightly outward and the B atoms were moved slightly inward from the tube center to make a buckled BNNT, which is consistent with previous ab initio calculations on BNNT geometries.[16,17] We also considered an open-ended (6,6) CNT with a length of about 14 Å to compare water behavior in similar diameter CNT and BNNT. The initial C−C and C−H bond lengths for the CNT were 1.42 and 1.09 Å, respectively. We then obtained geometry-optimized structures for the BNNTs and the CNT by the AM1 semiempirical method using HyperChem 7.51.[18] For BNNT geometries, the AM1 method reproduces the large cubic BN cluster in good agreement with the experimental structure.[19] For the CNTs, Han and Jaffe[20] found good agreement in carbon nanoconic tip energies and geometries obtained from using the AM1 and DFT/B3LYP methods. Furthermore, a CNT geometry obtained from the B3LYP/3-21G method has been found to be in good agreement with experiments.[21] To investigate the effect of the polarization of BNNT on water behavior and vice versa, we performed DFT calculations with and without water molecules inside the tubes. Gaussian 03[22] was used for the DFT calculations with B3LYP/6-31G** on the geometry-optimized structures. The partial charges on the tubes were obtained by fitting the electrostatic potential to a fixed charge on the B, N, C, and H atoms using the CHelpG scheme.[23] The CHelpG charges based on a molecular electrostatic potential are suited for MD simulations as they can capture higher-order effects arising from dipoles and mulipoles, though in an approximate way.

MD simulations were performed using modified GROMACS 3.3.1.[24] The MD domain consists of a nanotube, water, and a slab. A nanotube is fixed in a slab, and it connects two water reservoirs in contact with ends of the nanotube. The B and N atoms in a BNNT and C atoms in a CNT are modeled as uncharged Lennard-Jones particles. The extended simple point charge (SPC/E) model[25] with an oxygen atom of $-0.8476e$ charge and the two hydrogen atoms of $+0.4238e$ charge was used in the simulations. The SETTLE algorithm was implemented to constrain the OH bond length and the HOH bond angle at 1.0 Å and 109.47°, respectively. The SPC/E model has been used successfully in simulating water in complex biomolecular environments such as gramicidin channels with single water wires.[26] The simulation box ranges from $2.8 \times 2.772 \times 5.98$ to $4.4 \times 4.157 \times 7$ nm^3, depending on the size of the nanotube. The system was replicated periodically in all the three dimensions. The simulation box contained approximately 900−2500 water molecules depending on the simulation box size. The simulation was performed at a constant temperature of 300 K and a constant pressure of 1 bar. The Nosé-Hoover thermostat[27] with a time constant of 0.1 ps was employed to regulate the temperature at 300 K. The Parrinello-Rahman piston-coupling scheme[28] with a time constant of 2.0 ps and a compressibility of 4.5×10^{-5} bar^{-1} maintained the system at 1 bar. The Lennard-Jones parameters for B atoms, N atoms, H atoms, C atoms, water molecules, and slab are summarized in previous papers.[14,29] The particle mesh Ewald (PME) method with a 10 Å real-space cutoff, 1.5 Å reciprocal space gridding, and splines of order 4 with a 10^{-5} tolerance was implemented to compute electrostatic interactions. The equations of motion were integrated by using a leapfrog algorithm. After 1ns of equilibration time, the simulations were continued for another 28 ns to obtain enough statistical sampling to calculate the transport properties.

3. Results and Discussions

3.1. Partial Charges. Figure 1 shows CHelpG partial charges for a (5,5) BNNT. The positive (on B atoms) and negative charges (on N atoms) at the same axial positions are plotted separately in Figure 1a. Figure 1b shows the averaged partial charges for the atoms with the same axial position. As expected, the boron atoms with a lower electronegativity compared to the nitrogen atoms are positively charged while the nitrogen atoms are negatively charged in B−N bonding. H atoms forming dangling bonds with B and N atoms at the end of a tube have either positive or negative charges depending on which atoms the H atoms bind to (see Figure 1 and Table 1). We found a good agreement between the partial charges for H atoms with previous DFT calculations for H atoms bonding with a B−N cluster.[30] We also compared the partial charges on a finite-length BNNT with the partial charges on a finite-length CNT. The magnitude of the partial charges in a finite-length CNT decreases rapidly within a distance of about 2 Å.[29] Thus, the dominant contribution to the partial charges for the (6,6) single-walled CNT is from the end effects. Our preliminary studies on the calculation of partial charges for the (6,6) single-walled CNT saturated with H atoms also confirms the end effect. The magnitude of the averaged partial charges for atoms at the ends of a BNNT is higher than that in the middle of tube. Thus, the end effect is also observed in BNNT (see Figure 1b). However, in contrast to a CNT, Figure 1a indicates that an individual atom in a BNNT has a much higher magnitude of partial charge.

We also studied the effect of water on the electrostatic behavior of a BNNT. To investigate the effect of water molecules on the tube partial charges, we performed DFT calculations based on four different representative configurations obtained from equilibrium MD simulations that consisted of the nanotube and water molecules inside the tube and near the tube entrance. Two of the configurations were obtained from the MD simulations without partial charges on the atoms. The other two configurations were obtained by including partial charges on the atoms in MD simulations. Due to the inhomogeneous distribution of water molecules along the tube axial direction, the partial charge distribution is not quite symmetric with respect to the center of the nanotube. Table 1 shows a comparison of averaged partial charges for B and N atoms located in the middle of various size tubes. The partial charges obtained without including water molecules are comparable in all cases and are approximately $\pm 0.40e$. When water molecules are included in the calculations, as shown in Figure 1a and Table 1, the partial charges on B and N atoms increase significantly. Even though the partial charges on individual atoms are significantly different when water molecules are included, the averaged partial charges at an axial location (see Figure 1b) are not very different from those obtained without water molecules.

3.2. Single-File Water Chains. The use of atomic partial charges in molecular dynamics to improve the Lennard-Jones force field for water−boron/nitrogen interaction is essential. Our method of using one-way coupling between quantum and

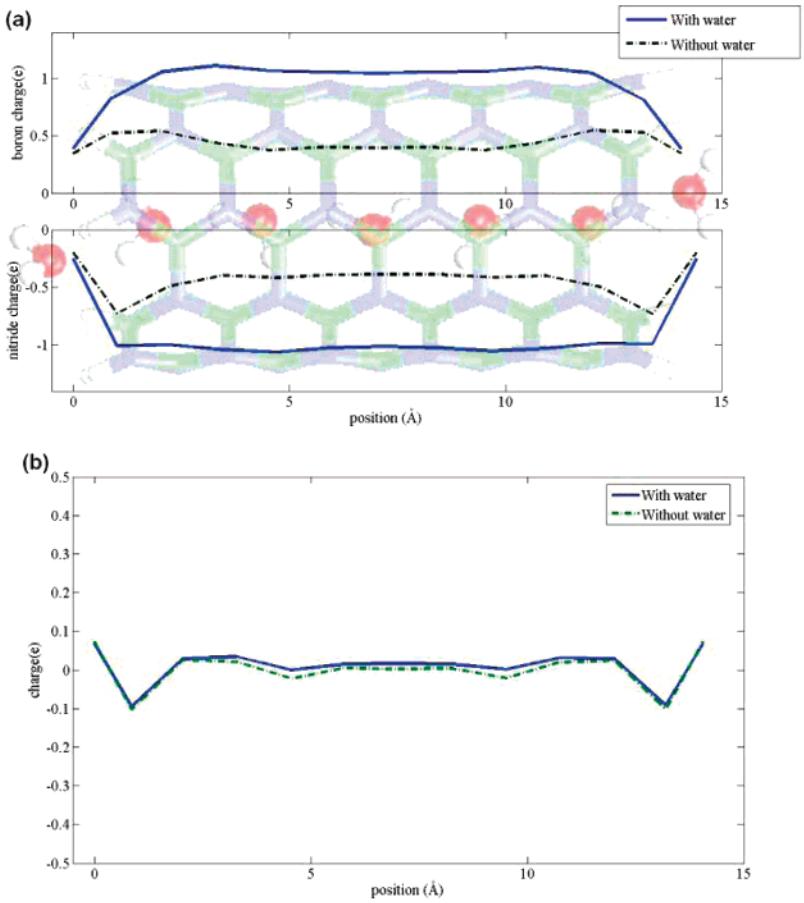

Figure 1. Visualization of (5,5) BNNT with water (shade), (a) partial charge distribution on boron atoms of (5,5) BNNT (top) and nitrogen atoms of (5,5) BNNT (bottom). (b) Partial charge distribution for atoms on a (5,5) BNNT along the tube axial direction. Solid line: water is included in the calculation; dashed line: no water is included in the calculation. A tube starts at 0 Å in the axial direction.

TABLE 1: Comparison of Averaged Partial Charges for B and N Atoms in the Middle of the BNNTS[a]

	(5,5) BNNT		(6,6) BNNT		(9,9) BNNT		(10,10) BNNT	
	w/o-Wt	w/Wt	w/o-Wt	w/Wt	w/o-Wt	w/Wt	w/o-Wt	w/Wt
B[*e*]	0.40	1.05	0.39	0.76	0.37	0.86	0.37	0.88
N[*e*]	−0.40	−1.05	−0.39	−0.76	−0.37	−0.86	−0.37	−0.88
H−B[*e*]	0.34	0.39	0.37	0.38	0.32	0.38	0.32	0.38
H−N[*e*]	−0.20	−0.25	−0.24	−0.25	−0.19	−0.24	−0.19	−0.24

[a] The partial charge of the H-atom connecting to the B-atom is denoted by H−B, and the partial charge of the H-atom connecting to the N-atom is denoted by H−N. w/o-Wt refers to without water, and w/Wt refers to with water.

molecular dynamics was evaluated in the previous study.[29] We found a similar water dipolar orientation inside a (6,6) CNT between ab initio MD simulation and classical MD simulation with partial charges, which suggests that the MD simulations with the partial charges could provide results similar to those with ab initio MD simulations.

Here, we investigate the single-file water chain behavior inside BNNTs. We first discuss the effect of partial charges on a (5,5) BNNT, and then we compare the behavior of a single-file chain inside a partially charged (5,5) BNNT, (5,5) CNT, (6,6) BNNT, and (6,6) CNT. The MD simulations were started with empty nanotubes. Our previous study[14] showed that water from the water reservoir filled an uncharged empty (5,5) BNNT within 40 ps. Water molecules in the nanotubes adopt a single-file formation, similar to the water structure in a biological water channel.[31] During the entire simulation time, there was a small fluctuation in the filling behavior for the uncharged (5,5) BNNT. The openness ω of the nanotube for water conduction based on water density was defined in the previous study.[14] We assign $\omega(t) = 1$ (open) when water density in the tube at any instant is greater than 50% of the density of a completely filled tube. The tube is closed ($\omega(t) = 0$), otherwise. The average openness, $\langle\omega\rangle = T_{open}/T_{simulation}$, of the uncharged (5,5) BNNT is 0.986. When the partial charges are introduced in the system, the wetting behavior of the (5,5) BNNT has improved, that is, once an initially empty (5,5) BNNT with partial charges was filled with water molecules, the nanotube remained to be open for water conduction during the rest of the simulation time (see Figure 2a). The average openness for the (5,5) BNNT increases to 0.992 in the presence of partial charges. For an uncharged (5,5) BNNT, similar to an uncharged (6,6) CNT,[29] all the water molecules in the tube orient such that the dipole vectors of the water molecules point either toward the top water reservoir or toward the bottom water reservoir at any instant. Figure 3a shows that when a water molecule in a single-file chain flips and reverses its orientation, the strong electrostatic coupling leads to simultaneous flipping of all other water molecules in the chain. The partial charges of a (5,5) BNNT induce a significant change in the water structure, that is, while the water dipoles at both ends of the tube are oriented toward their

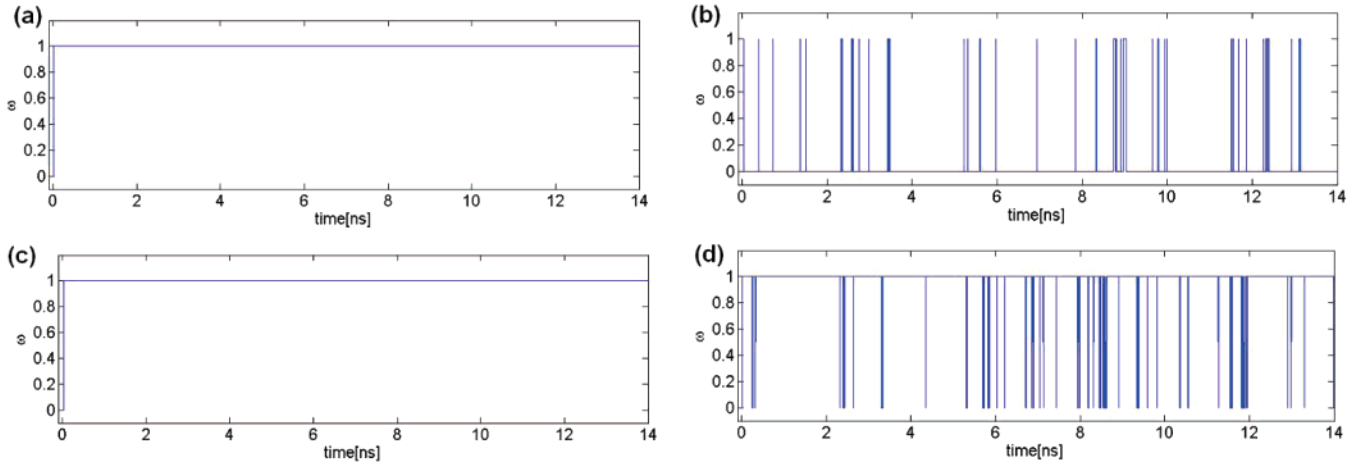

Figure 2. The openness ω of a partially charged (5,5) boron nitride nanotube (a), (5,5) carbon nanotube (b), (6,6) boron nitride nanotube (c), and (6,6) carbon nanotube for water conduction.

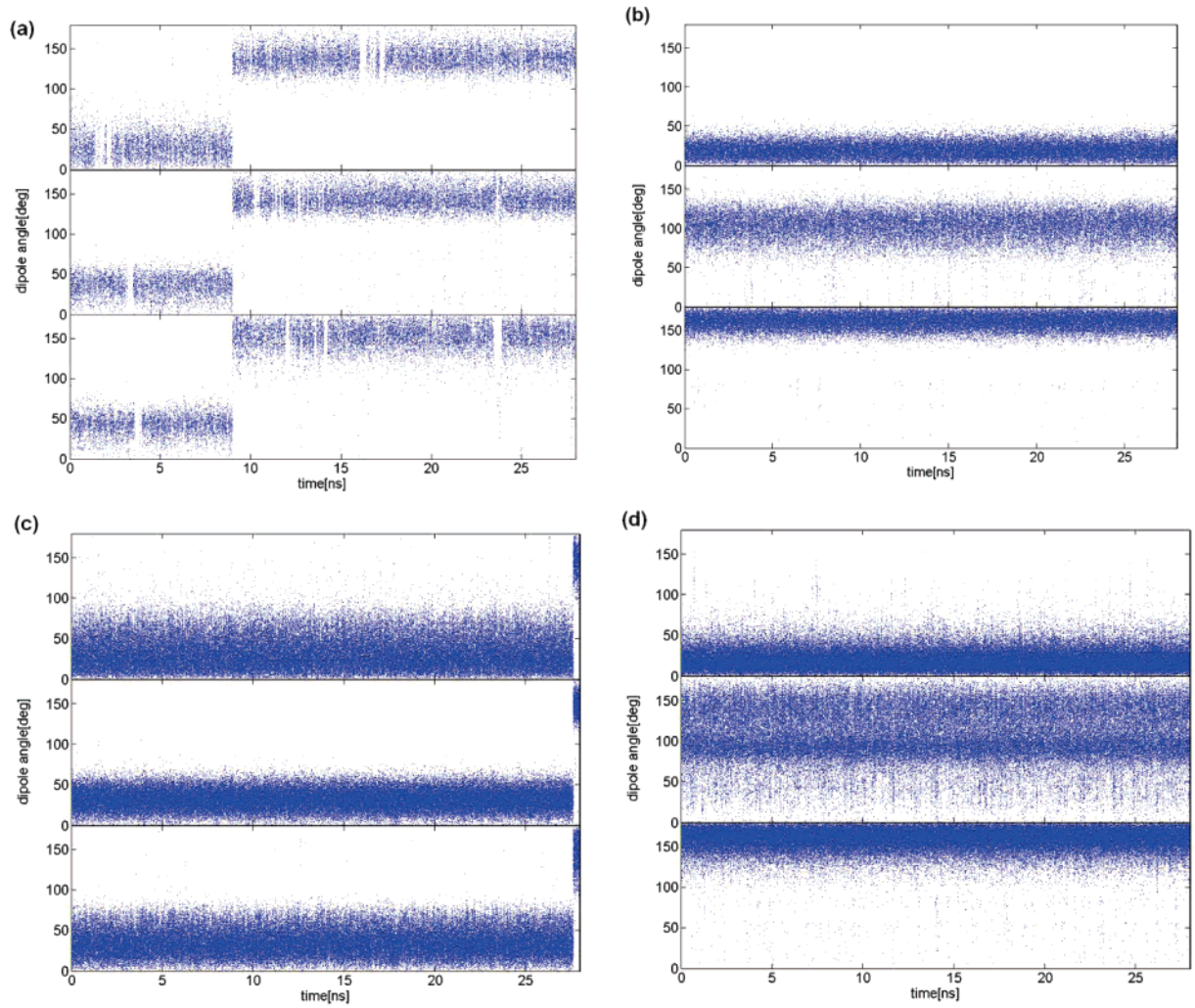

Figure 3. Transient of water dipole orientation in (a) an uncharged (5,5) BNNT, (b) a partially charged (5,5) BNNT, (c) an uncharged (6,6) BNNT, and (d) a partially charged (6,6) BNNT. The top, middle, and bottom rows indicate the orientation of water molecules in the top (1.8 nm from the top end), middle (0.5−0.68 nm), and bottom (1.8 nm from the bottom end) regions of the tube, respectively. The water dipole orientation angle is defined as the angle between the water dipole vector and the tube axis *z*. 0° denotes the water dipole vector pointing toward the positive *z*-axis. 90° denotes the water dipole vector pointing normal to the tube axis.

respective reservoirs, the central water molecule forms an *L*-defect.[32] This observation is similar to the formation of an *L*-defect inside a (10,0) CNT with partial charges.[29]

Figure 2, parts a and c, shows the superior filling behavior of a BNNT, which results from a strong nitrogen−water van der Waals attraction,[14] and the BNNT−water electrostatic interaction. The carbon−water interaction is not strong enough for the (5,5) CNT to have continuous filling of water molecules, and the atomic partial charges of the (5,5) CNT cannot drastically improve its wetting behavior (Figure 2b). Figure 2d shows that the filling behavior is favorable for a partially charged (6,6) CNT. Even though the wetting behavior has improved

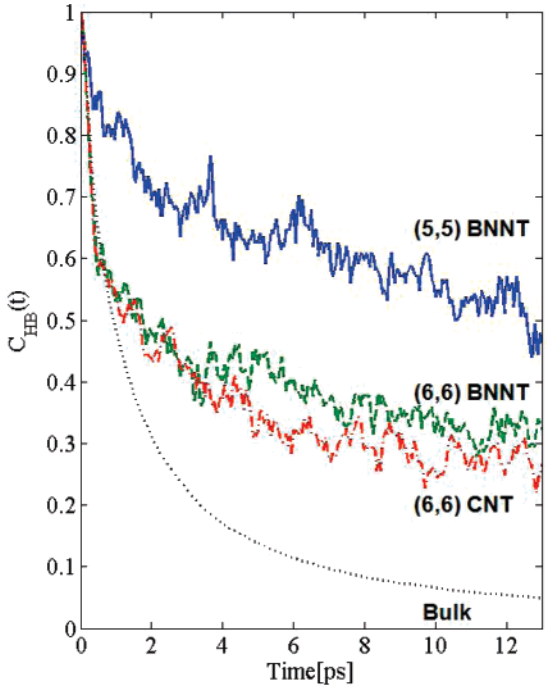

Figure 4. Hydrogen bonding autocorrelation function $C_{HB}(t)$ for a water−water hydrogen bond inside a partially charged nanotube.

significantly as the diameter of the nanotube increased, the (6,6) CNT was still found to be closed for water conduction for short periods of time. The dipole orientation of a single-file chain can also be considerably affected by the type of the nanotube and its diameter as shown in Figure 3. Similar to the observation in the (5,5) BNNT with partial charges, an *L*-defect was also observed in the single-file water chain in the partially charged (6,6) BNNT. The partially charged (5,5) BNNT and (6,6) BNNT have similar water structure, but water molecules inside a partially charged (5,5) BNNT have a smaller fluctuation in the dipolar angle compared to those inside a partially charged (6,6) BNNT. Unlike in BNNTs, all the water molecules inside the partially charged (6,6) CNT point either toward the top or the bottom water reservoir, and the water dipole flips continuously.[29] These observations can be understood in more detail by analyzing the hydrogen-bonding dynamics of water molecules inside the nanotubes.

The strong and directional hydrogen bonding of water play a key role in the peculiar properties of water molecules. The water−water hydrogen bond can be defined using a geometrical criterion.[33] For a pair of water molecules, the hydrogen atom forms the hydrogen bond if the following two conditions are simultaneously fulfilled: (1) the distance between oxygen atoms is less than 3.5 Å, $R_{OO} < 3.5$ Å, this is the first minimum position on the oxygen−oxygen radial distribution function; (2) the angle between the O−O vector and the O−H vector does not exceed 30°. The hydrogen bond dynamics can be characterized by an autocorrelation of the hydrogen bond population, called the hydrogen bond autocorrelation function (HBACF):[33,34]

$$C_{HB}(t) = \frac{\langle h(0)h(t)\rangle}{\langle h(0)\rangle} \tag{1}$$

where $h(t)$ is a hydrogen bond population descriptor for each pair of water molecules, and $h(t) = 1$ if a tagged pair of molecules is hydrogen bonded at time t and, $h(t) = 0$, otherwise. This autocorrelation function describes the probability that the tagged pair of water molecules form hydrogen bonding at time t given that the pair was hydrogen bonded at time zero.

TABLE 2: Comparison of Axial Water Diffusion Coefficient D_z and Percentage of Water Forming Water−Nitrogen Hydrogen Bonds When the Oxygen−Nitrogen Distance Is Less than 3.5 Å in a Boron Nitride Nanotube

chirality	diameter [Å]	charge type	D_z [10^{-5} cm^2/s]	% of H-bond$_{Wt}$−N
(5,5)	6.9	no partial charge	1.18 ± 0.06[14]	0
(5,5)	6.9	partial charge	1.15 ± 0.04	15.74
(6,6)	8.2	no partial charge	1.29 ± 0.02	0
(6,6)	8.2	partial charge	1.25 ± 0.03	7.96
(9,9)	12.2	no partial charge	0.63 ± 0.02	0
(9,9)	12.2	partial charge	0.68 ± 0.03	4.30
(10,10)	13.6	no partial charge	1.28 ± 0.04	0
(10,10)	13.6	partial charge	0.93 ± 0.06	4.13

Figure 4 shows a comparison of HBACF for water molecules inside the partially charged (5,5) BNNT, (6,6) BNNT, and (6,6) CNT. Figure 4 suggests that water molecules in the partially charged (5,5) BNNT form rigid hydrogen bonding and the hydrogen bonding is maintained longer when compared to other tubes. Therefore, the highly ordered water structure with a strong hydrogen-bonding network in the (5,5) nanotube induces continuous tube opening for water conduction and a smaller deviation in the water dipolar angle. On the other hand, the hydrogen bonds between water molecules in a partially charged (6,6) CNT are more rigid compared to the bulk, but more flexible compared to those in the partially charged (5,5) and (6,6) BNNTs. Its intermittent wetting behavior and the continuous flipping can be understood by the frequent water−water hydrogen-bonding breakage together with the relatively weak carbon−water interaction.

3.3. Anomalous Water Behavior. The radial density distribution function, $g(r)$, provides quantitative information about water interactions in BNNTs. Figure 5 shows the $g(r)$ of water molecules as a function of tube diameter and partial charges. Similar to the structure of water in CNTs,[35,36] the structure of confined water is strongly affected by the diameter of the BNNT. For uncharged BNNTs, water molecules inside the (9,9) BNNT with a diameter of 12.18 Å form an ice-shell structure, analogous to the anomalous ice-like behavior in both symmetry and mobility in a (9,9) CNT.[36] In a (10,10) BNNT, it was observed that an additional single-file water chain formed inside the surrounding ice-shell structure. When partial charges are introduced in the system, the B and N atoms having a relatively high magnitude of partial charge attract water molecules to stretch the ice-shell toward the tube wall. This tiny adjustment of the ice-shell structure in a radial location inside the partially charged (9,9) BNNT creates room inside the ice-shell structure to form an inner single-file chain. Since the attraction between ice-shell and the nanotube is not strong enough, only an intermittent single-file chain of water was observed.

The transport properties of confined water can vary with diameter as the properties have a strong correlation with the water structure. In the present study, we evaluated the transport properties by computing the self-diffusion coefficient. Since water conducts through the BNNTs by forming a single-file chain and/or a cylindrical structure, we considered only water diffusion in the axial direction.

The axial diffusion coefficient D_z of water is related to the slope of the water mean-squared displacement (MSD) by the well-known Einstein relation,

$$D_z = \frac{1}{2}\lim_{t\to\infty}\frac{\langle |r(t) - r(0)|^2\rangle}{\Delta t} = \frac{1}{2}\lim_{t\to\infty}\frac{\langle \Delta r^2\rangle}{\Delta t} \tag{2}$$

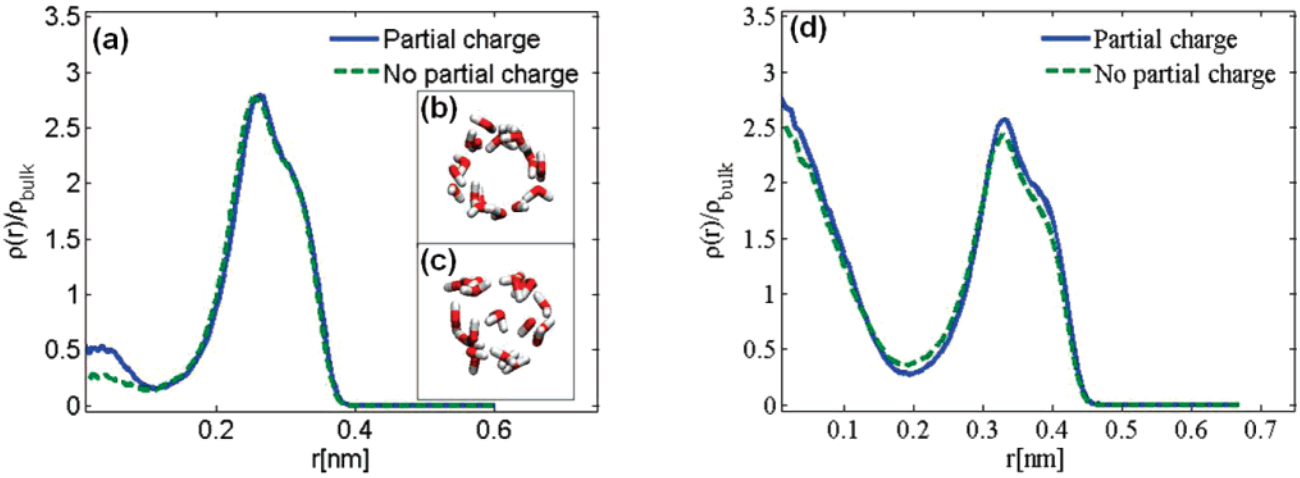

Figure 5. Radial density profile $\rho(r)$ inside a (9,9) BNNT (a), and a (10,10) BNNT (d). Cross-sectional view of water inside an uncharged (9,9) BNNT (b), and a partially charged (9,9) BNNT (c) showing a multi-columnar water structure.

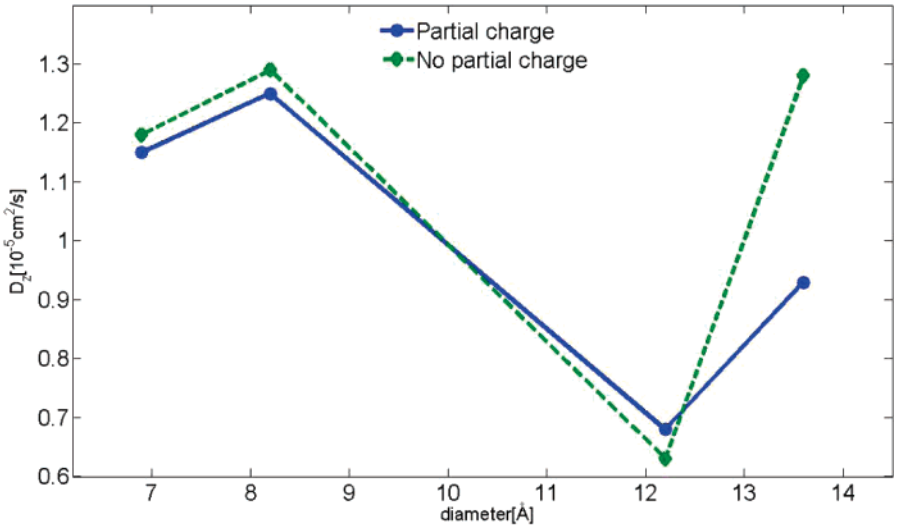

Figure 6. Averaged axial diffusion coefficient of water (D_z) inside BNNTs.

where $r(t)$ is the position vector at time t. Table 2 and Figure 6 show the anomalous diffusion of water in BNNTs of various nanotube diameters. The diffusion coefficient of water inside the BNNTs is significantly less than that in the bulk, 2.69×10^{-5} cm^2/s.[36] This observation suggests that water diffusion is influenced by the water structure inside the BNNTs. In the case of a single-file water chain (i.e., in (5,5) BNNT and (6,6) BNNT), the diffusion coefficient of water in the tube is approximately 1.2×10^{-5} cm^2/s. It decreases drastically for a (9,9) BNNT with a critical diameter of 12.18 Å where anomalous immobilization occurs due to the highly ordered lattice (ice-like water structure). The axial diffusion coefficient of water increases in the (10,10) BNNT where an inner single-file chain surrounded by a cylindrical water structure is observed. Partial charges induce a considerable change in the water diffusion coefficient. Water molecules in a partially charged (5,5) BNNT have about 2.54% lower diffusion coefficient compared to water molecules in an uncharged nanotube. Similarly, a lower diffusion coefficient was found for water in (6,6) and (10,10) BNNTs with partial charges. In the case of a partially charged (9,9) BNNT, however, the water diffusion coefficient increases, compared to uncharged (9,9) BNNT. The decrease in the axial diffusion coefficient of water with partial charges is in contrast to the previous study on the effect of partial charge on water dynamics inside a carbon nanotube.[29] The study suggested that the diffusion coefficient of water inside a carbon nanotube increases because partial charges reduce the water permeation barrier. This unique and interesting diffusion behavior of water inside a BNNT can be understood by examining the hydrogen bonding between water and nitrogen atoms on the tubes.

In the case of BNNT, the magnitude of the partial charge on an individual nitrogen atom is relatively high compared to that of C atoms on a CNT. We thus considered the possibility of forming hydrogen bonding between the confined water and the N atoms. To determine the water−nitrogen hydrogen bond, we used an energetic definition, which considers the water and nitrogen to be bonded if the nitrogen−oxygen distance is less than 3.5 Å, $R_{NO} < 3.5$ Å, and their interaction energy is less than threshold energy of −18.32 kJ/mol (this value is taken from recent DFT calculations on hydrogen bond energy between H_2O and NH_3.[37]) Table 2 shows the percentage of water forming water−nitrogen hydrogen bonds when water molecules inside the nanotube are close enough to the tube wall to satisfy the R_{NO} criteria. We found that there is no hydrogen bond between nitrogen and water in the case of an uncharged BNNT. A water−nitrogen hydrogen bond forms only if a BNNT is partially charged. Even though the number of nitrogen−water hydrogen bonds is small, the attraction between water and nitrogen atoms arising from the hydrogen bonds can improve the filling behavior but interrupt the axial motion of water molecules. Therefore, partially charged (5,5), (6,6), and

(10,10) BNNTs have a slightly lower water axial diffusion coefficient compared to that of the uncharged nanotubes. In the case of a (9,9) BNNT, however, the axial diffusion coefficient of water increases with partial charges. This anomalous water diffusion behavior can be explained by the significant water structure change (from an ice-shell structure to an ice-shell structure surrounding a single-file chain). The presence of an inner single-file chain increases the axial diffusion coefficient of water in a partially charged (9,9) BNNT. The axial diffusion of water inside a partially charged (9,9) BNNT is still slower than a (10,10) BNNT because the chance of forming a single-file chain inside an ice-shell structure for a partially charged (9,9) BNNT is much lower than that for a (10,10) BNNT.

4. Conclusions

In this work, we have investigated the effect of partial charges on the structure and transport properties of water confined in BNNTs of various diameters using combined DFT and molecular dynamics (MD) simulations. DFT calculations reveal that B and N atoms in a BNNT have a higher magnitude of partial charges compared to that of carbon atoms in a CNT. We observed that the wetting behavior of a (5,5) BNNT has improved in the presence of partial charges. The wetting behavior of water inside a subnanometer BNNT is better than that of a CNT with a similar diameter. Once water molecules filled an initially empty partially charged (5,5) BNNT, the (5,5) BNNT remained open for water conduction during the entire simulation time, while a partially charged (5,5) CNT does not conduct water molecules. An *L*-defect was observed inside a partially charged (5,5) BNNT and (6,6) BNNT. The single-file chain structure is more rigid in a partially charged (5,5) BNNT than in a partially charged (6,6) BNNT due to the relatively sturdy hydrogen bonds between water molecules in the (5,5) BNNT. The water diffusion and structure are modified by the diameter of the BNNT—similar to the behavior reported in a CNT.[36] Confinement causes a considerably slower diffusion of water compared to bulk. Water molecules in partially charged (5,5), (6,6), and (10,10) nanotubes have a lower diffusion coefficient compared to that in uncharged tubes. The formation of hydrogen bonds between nitrogen atoms on the tube and water molecules induces slower water diffusion with partial charges. Finally, anomalous water behavior was found in a (9,9) BNNT. An ice-shell water structure forms inside the uncharged (9,9) nanotube with a critical slowing of water diffusion. In the presence of partial charges, an occasional single-file water chain is observed inside the ice-shell water structure, which results in an increase in the water diffusion coefficient.

Acknowledgment. This research was supported by NSF under Grant Nos. 0328162, 0120978, 0523435, and 0625421 and by NIH under Grant No. PHS 2 PN2 EY016570B.

References and Notes

(1) Blasé, X.; Rubio, A.; Louie, S. G.; Cohen, M. L. *Europhys. Lett.* **1994**, *28*, 335.

(2) Chopra, N. G.; Luyken, R. J.; Cherrey, K.; Crespi, V. H.; Cohen, M. L.; Louie, S. G.; Zettl, A. *Science* **1995**, *269*, 966.; Suryavanshi, A. P.; Yu, M.; Wen, J.; Tang, C.; Bando, Y. *Appl. Phys. Lett*. **2004**, *84*, 2527.

(3) Hernández, E.; Goze, C.; Bernier, P.; Rubio, A. *Phys. Rev. Lett.* **1998**, *80*, 4502.

(4) Kudin, K. N.; Scuseria, G. E.; Yakobson, B. I. *Phys. Rev. B* **2001**, *64*, 235406.

(5) Chang, C. W.; Fennimore, A. M.; Afanasiev, A.; Okawa, D.; Ikuno, T.; Garcia, H.; Li, D.; Majumdar, A.; Zettl, A. *Phys. Rev. Lett.* **2006**, *97*, 085901.

(6) Khoo, K. H.; Mazzoni, M. S. C.; Louie, S. G. *Phys. Rev. B* **2004**, *69*, 201401.

(7) Zhi, C.; Bando, Y.; Tang, C.; Goldberg, D. *Phys. Rev. B* **2006**, *74*, 153413.

(8) Chen, Y.; Zou, J.; Campbel, S. J.; Caer, G. L. *Appl. Phys. Lett.* **2004**, *84*, 2430.

(9) Tsang, S. C.; Harris, P. J. F.; Green, M. L. H. *Nature (London*) **1993**, *362*, 520.

(10) Ajayan, P. M.; Ebbesen, T. W; Ichihashi, T.; Iijima, S.; Tanigaki, K.; Hiura, H. *Nature (London*) **1993**, *362*, 522.

(11) Hummer, G.; Rasaiah, J.; Noworya, J. P. *Nature (London*) **2001**, *414*, 188.

(12) Rafii-Tabar, H. *Phys. Rep.* **2004**, *390*, 235.

(13) Samson, M. S. P.; Biggin, P. C. *Nature (London*) **2001**, *414*, 156.

(14) Won, C. Y.; Aluru, N. R. *J. Am. Chem. Soc.* **2007**, *129*, 2748.

(15) Pauling, L *The Nature of the Chemical Bond*; Cornell University Press: Ithaca, NY, 1960.

(16) Wirtz, L.; Rubio, A. *Phys. Rev. B* **2003**, *68*, 045325.

(17) Akdim, B.; Pachter, R.; Duan, X.; Adams, W. W. *Phys. Rev. B* **2003**, *67*, 245404.

(18) HyperChem Professional 7.51; Hypercube, Inc., 1115 NW 4th Street, Gainesville, Florida 32601, USA.

(19) Komatsu, S.; Yarbrough, W.; Moriyoshi, Y. *J. Appl. Phys.* **1997**, *81*, 7798.

(20) Han, J.; Jaffe, R. *J. Chem. Phys*. **1998**, *108*, 2817.

(21) Sano, N.; Chhowalla, M.; Roy, D.; Amaratunga, A. *Phys. Rev. B* **2002**, *66*, 133493.

(22) Frisch, M. J.; Trudes, G. W.; Schlegel, H. B.; et al. *GAUSSIAN 03*, Revision C.02; Gaussian, Inc.: Wallingford, CT, 2004.

(23) Breneman, C. M.; Wiberg, K. B. *J. Comput. Chem.* **1990**, *11*, 361.

(24) Lindahl, E.; Hess, B.; van der Spoel, D. *J. Mol. Model.* **2001**, *7*, 306.

(25) Berendsen, H. J. C.; Grigera, J. R.; Straatsma, T. P. *J. Phys. Chem.* **1987**, *91*, 6269.

(26) Chiu, S.-W.; Subramaniam, S.; Jakobsson, E. *Biophys. J.* **1999**, *76*, 1939.

(27) Hoover, W. *Phys. Rev. A* **1985**, *31*, 1695.

(28) Parrinello, M.; Rahman, A. *J. Appl. Phys.* **1981**, *52*, 7182.

(29) Won. C. Y.; Joseph, S.; Aluru, N. R. *J. Chem. Phys.* **2006**, *125*, 114701.

(30) Han, S. S.; Kang, J. K.; Lee, H. M.; van Duin, A. C. T.; Goddard, W. A. *J. Chem. Phys.* **2005**, *123*, 114703.

(31) de Groot, B. L.; Grubmüller, H. *Curr. Opin. Struct. Biol.* **2005**, *15*, 176.

(32) Bjerrum, N. *Science* **1952**, *115*, 385; Best, R. B.; Hummer, G. *Proc. Natl. Acad. Sci. U.S.A* **2005**, *102*, 6732.

(33) Luzar, A.; Chandler, D. D. *Nature (London*) **1995**, *379*, 55.

(34) Luzar, A. *J. Chem. Phys.* **2000**, *113*, 10663.; Paul, S.; Chandra, A.; *Chem. Phys. Lett.* **2004**, *386*, 218.; Liu, P.; Harder, E.; Berne, B. J. *J. Phys. Chem. B* **2005**, *109*, 2949.

(35) Striolo, A.; Chialvo, A. A.; Gubbins, K. E.; Cummings, P. T. *J. Chem. Phys.* **2005**, *122*, 234712.

(36) Mashl, R. J.; Joseph, S. S.; Aluru, N. R.; Jakobsson, E. *Nano Lett.* **2003**, *3*, 589.

(37) Oliveira, B. G.; Pereira, F. S.; de Araújo, R. C. M. U.; Ramos, M. N. *Chem. Phys. Lett.* **2006**, *427*, 181.